Proceedings of the 36th Chinese Control Conference
July 26-28, 2017, Dalian, China

Neural Network Control of Lower Limb Rehabilitation Exoskeleton with Repetitive Motion

Deqing Huang[1], Lei Ma[1], YongYang[1]
1. Institute of Systems Science and Technology, Southwest Jiaotong University, Chengdu 610031, P. R. China
E-mail: elehd@home.swjtu.edu.cn

Abstract: This paper addresses neural network (NN) control of a lower limb exoskeleton for rehabilitation. Both the interaction between human and exoskeleton and external disturbances are considered. The controller is developed based on a combined scheme of repetitive learning control (RLC) and neural networks (NN), where RLC is used to learn periodic uncertainties (the interaction between human and exoskeleton) attribute to the repetitive motion of the exoskeleton leg, and NN is adopted to approximate all the external disturbances. Stabilities of the controllers are proved rigorously in a Lyapunov way. Simulations are worked out to illustrate the performance of the proposed control schemes.

Key Words: Rehabilitation exoskeleton, neural networks, repetitive learning control.

1 Introduction

Stroke patients often have to perform a large number of training during their rehabilitation therapy. In traditional assisted training, physiotherapists usually help patients to perform rehabilitation therapy manually [1]. This leads to some limitations, such as the dependence on the availability of skilled personnel, and possibility of providing high-intensity motor training under controlled conditions [2]. In recent years, development of robots for rehabilitation has received much attention to assist medical workers to perform a large amount of tedious repetitive movements [3–7].

Rehabilitation Exoskeleton is a type of representative robots to perform motion training [8–11]. Its working process can be described as follows. First, the stroke patient wears an exoskeleton on his or her limbs; Then, a control scheme is implemented on the exoskeleton segments to make them track some desired training trajectories, so that the limbs and the exoskeleton segments can be moved together. As there are frequent physical interactions between the patient's limbs and the exoskeleton segments, a well-designed control scheme is imperative to achieve efficient tracking performance and keep the security of human body.

In terms of exoskeleton control, several intelligent control schemes have been proposed and tested. In [12], a model-based compensation control framework was presented to support robot-aided shoulder-elbow rehabilitation and power assistance tasks for the developed upper body exoskeleton system. In [13], a patient-cooperative control strategy was implemented for ChARMin, which is the first actuated exoskeleton robot for pediatric arm rehabilitation. The controller enables free arm movements, assistance-as-needed, and complete guidance of the arm. In [14], an electromyogram(EMG)-based impedance control method for an upper-limb power-assist exoskeleton robot is proposed to control the robot in accordance with the user's motion intention, and a neurofuzzy matrix modifier is applied to make the controller adaptable to any users. In [15], by introducing a low-pass-filter, an inertia compensation controller was proposed for a one-degree-of-freedom exoskeleton, where the controller combines two assistive effects: increasing the natural frequency of the lower limbs and performing net work per swing cycle. It is worthy of pointing out that all the aforementioned controllers lose sight of the repetition characteristics of the exoskeleton system, which play a crucial role in rehabilitation therapy.

As simple mathematical models of biological neural networks, artificial neural networks (NNs) have been widely used in the control of robot systems [16, 17], and exoskeletons [18–20]. In [21], an adaptive NN controller for dual-arm coordination of a humanoid robot with unknown nonlinearities in output mechanism has been proposed. In [22], adaptive NNs are used to approximate the unknown model of a rehabilitation robot. In [23], an inverse nonlinear controller, combined with an adaptive NN proportional integral (PI) sliding mode using an on-line learning algorithm, was proposed for a unicycle-like mobile robot. In [24], cerebellar model arithmetic computer NNs are used to design controllers for a robotic manipulator in the presence of large modeling uncertainties and external disturbance.

Rehabilitation exoskeletons are among the many robot control systems that are subject to uncertainties, such as interaction between human and exoskeleton, and external disturbances. It is clear that the exoskeleton systems have the characteristics of repetitive motion during the rehabilitation therapy. Hence, it is rational to consider the uncertainties of the exoskeleton systems as two parts, the periodic part and the non-periodic part. In principle, the periodic part is mainly caused by the interactions between wearer and exoskeleton, while the non-periodic part consists of external disturbances such as frictional forces with the ground.

As an effective learning-type controller in dealing with repetitive control tasks or systems with periodic characteristics [25]-[29], repetitive learning control (RLC) has been widely used in many fields[30–34]. The aim of this paper is to address the tracking control of rehabilitation exoskeleton, where a combination of NN and repetitive learning control (RLC) are considered. A combined error factor (CEF), which consists of the weighted sum of tracking error and its derivative, is adopted to facilitate the convergence analysis. Stability of the proposed controller is proved rigorously in a Lyapunov way.

This work is supported by National Natural Science Foundation (NNSF) of China under Grant 61640310.

This paper is organized as follows. Problem formulation and preliminaries are given in Section II,. Section III addresses controller design and stability analysis. In Section IV, the performance of the proposed controller is verified by simulations. Section V concludes the work.

2 Problem Formulation and Preliminaries

2.1 Problem Formulation

The dynamics of an n-link lower limb exoskeleton can be described as

$$M(\boldsymbol{\theta})\ddot{\boldsymbol{\theta}}+C(\boldsymbol{\theta},\dot{\boldsymbol{\theta}})\dot{\boldsymbol{\theta}}+G(\boldsymbol{\theta})=\boldsymbol{\tau}+F(t)+\Delta \tag{1}$$

where $\boldsymbol{\theta}\in R^{n\times 1}$, $\dot{\boldsymbol{\theta}}$, and $\ddot{\boldsymbol{\theta}}$ are vectors of the generalized coordinates, the velocities, and the accelerations respectively, and $\boldsymbol{\tau}\in R^{n\times 1}$ is the vector of torques acted on the exoskeleton joints, which is the actual control input to exoskeleton. $M(\boldsymbol{\theta})\in R^{n\times n}$ is a positive-definite and symmetric inertia matrix, $C(\boldsymbol{\theta},\dot{\boldsymbol{\theta}})\in R^{n\times n}$ is related to the centrifugal and Coriolis terms, and $G(\boldsymbol{\theta})\in R^{n\times 1}$ is the gravity term. $F(t)$ denotes the interactions between wearer and exoskeleton, and Δ denotes the external disturbance and frictional forces.

The following properties hold for system (1) [36].

Property 1. The inertia matrix $M(\boldsymbol{\theta})$ is symmetric and positive, which is further bounded:

$$\lambda_1\|\boldsymbol{x}^2\|<\boldsymbol{x}^T M(\boldsymbol{\theta})\boldsymbol{x}<\lambda_2\|\boldsymbol{x}^2\|,\ \forall \boldsymbol{x},\boldsymbol{\theta}\in R^n, \tag{2}$$

where λ_1 and λ_2 are positive constants.

Property 2. The centrifugal and Coriolis matrix $C(\boldsymbol{\theta},\dot{\boldsymbol{\theta}})$ and the time derivative of the inertia matrix $M(\boldsymbol{\theta})$ satisfy

$$\boldsymbol{x}^T[\dot{M}(\boldsymbol{\theta})-2C(\boldsymbol{\theta},\dot{\boldsymbol{\theta}})]\boldsymbol{x}=0,\ \forall \boldsymbol{x},\boldsymbol{\theta},\dot{\boldsymbol{\theta}}\in R^n. \tag{3}$$

Property 3. The non-periodic uncertainties $\Delta(t,\boldsymbol{\theta},\dot{\boldsymbol{\theta}},\ddot{\boldsymbol{\theta}})$ is bounded by δ, i.e.,

$$\|\Delta\|<\delta, \tag{4}$$

where $\delta>0$ is a known positive constant.

The control task for the rehabilitation exoskeleton system can be summarized in the following: given the desired training trajectories $\boldsymbol{\theta}_d$, the control objective is to synthesize bounded control inputs $\boldsymbol{\tau}$ such that the output trajectories of the exoskeleton $\boldsymbol{\theta}$ can track $\boldsymbol{\theta}_d$ as closely as possible in spite of various model uncertainties and disturbances.

2.2 Preliminaries

A RBF NN with n inputs, k outputs and p hidden units can be expressed as [37]

$$h_i(\boldsymbol{x})=\exp\left[-\frac{\|\boldsymbol{x}-\boldsymbol{c}_i\|^2}{2{\sigma_i}^2}\right], \tag{5}$$

$$y_i=\sum_{j=1}^{p} w_{ij}h_j,\ i=1,2,\cdots,k, \tag{6}$$

where $\boldsymbol{x}\in R^n$ is the input of NN, $h_i(x)\in R$ is the output of the ith hidden layer, and $y_i\in R$ is the ith output of the NN. Moreover, $w_{ij}\in R$ is the weight for the jth hidden layer to the ith output of NN, $\boldsymbol{c}_i\in R^n$, $\sigma_i>0$ are the centre and the width of the ith kernel unit, respectively. Let

$$\hat{W}=\begin{bmatrix} w_{11} & w_{21} & \cdots & w_{k1}\\ w_{12} & w_{22} & \cdots & w_{k2}\\ \vdots & \vdots & \vdots & \vdots\\ w_{1p} & w_{2p} & \cdots & w_{kp}\end{bmatrix} \tag{7}$$

$$H(\boldsymbol{x})=\begin{bmatrix} h_1(\boldsymbol{x})\\ h_2(\boldsymbol{x})\\ \vdots\\ h_p(\boldsymbol{x})\end{bmatrix}, Y=\begin{bmatrix} y_1\\ y_2\\ \vdots\\ y_p\end{bmatrix}. \tag{8}$$

The approximation of the NN can be rewritten in a compact form,

$$Y=\hat{W}^T H(\boldsymbol{x}). \tag{9}$$

RBF NNs are widely used to approximate unknown nonlinearities due to their inherent approximation capabilities. When the unknowns to be approximated, denoted by $\Lambda(\boldsymbol{x}): R^n\to R^k$, are piecewise continuous, the following is assumed to be true unconditionally.

Assumption 1 [38]. Assume that there exists a parametric matrix $W^*\in R^{p\times k}$, known as the optimal approximation parameter, such that ${W^*}^T H(\boldsymbol{x})$ can approximate the system unknows as close as possible, that is, given an arbitrary small positive constant ε_N, there exists an optimal weight matrix W^* so that the approximation error $\varepsilon(\boldsymbol{x})={W^*}^T H(\boldsymbol{x})-\Lambda(\boldsymbol{x}): R^n\to R^k$ satisfies

$$\|\varepsilon(\boldsymbol{x})\|=\|{W^*}^T H(\boldsymbol{x})-\Lambda(\boldsymbol{x})\|<\varepsilon_N. \tag{10}$$

The following lemma is used for the following state.

Lemma 1.[39] Let $P_i(t)\in P(t)$, $\hat{P}_i(t)\in\hat{P}(t)$, $\widetilde{P}_i(t)\in\widetilde{P}(t)$, $f(t)\in R$, and assume the following relations hold

$$\begin{aligned} P_i(t)(t)&=P_i(t)(t-T)\\ \widetilde{P}_i(t)&=P_i(t)-\hat{P}_i(t)\\ \hat{P}_i(t)&=\hat{P}_i(t-T)+f(t)\end{aligned} \tag{11}$$

Then the upper right-hand derivative of

$$\int_{t-T}^{t}\widetilde{P}_i^2(\mu)d\mu$$

is

$$-2\widetilde{P}_i f(t)-f^2(t)$$

3 Controller Design and Convergence Analysis

In this section, a controller scheme will be developed to address the control problem of lower limb exoskeleton for rehabilitation. To facilitate the controller design and its analysis, a combined error factor is first introduced.

$$E(t)=k_1\boldsymbol{e}(t)+k_2\dot{\boldsymbol{e}}(t) \tag{12}$$

where $\boldsymbol{e}(t)=\boldsymbol{\theta}(t)-\boldsymbol{\theta}_d(t)$, $\dot{\boldsymbol{e}}(t)=de/dt$, and $k_1,k_2>0$ are the weight factors of the combined error.

Now, we are in the position of deriving the tracking error dynamics of the exoskeleton. Assume that the control input $\boldsymbol{\tau}$ takes the following form,

$$\boldsymbol{\tau}=M(\boldsymbol{\theta})\ddot{\boldsymbol{\theta}}_d+C(\boldsymbol{\theta},\dot{\boldsymbol{\theta}})\dot{\boldsymbol{\theta}}_d+G(\boldsymbol{\theta})+\boldsymbol{u} \tag{13}$$

where $\boldsymbol{u}$ is the virtual input to be designed later. Substituting (13) into the system dynamics (1), we have

$$M(\boldsymbol{\theta})\ddot{e}(t)+C(\boldsymbol{\theta},\dot{\boldsymbol{\theta}})\dot{e}(t)=\boldsymbol{u}+F(t)+\Delta \tag{14}$$

Without loss of generality, assume that the interactions between the wearer and exoskeleton, $F(t)$, is periodic in time, namely, there exists a constant $T>0$ such that

$$F(t)=F(t-T). \tag{15}$$

The proposed controller that combines NNs and RLC is given as follows.

$$\begin{aligned}\boldsymbol{u}=&-\frac{k_1}{k_2}M(\boldsymbol{\theta})\dot{\boldsymbol{e}}(t)-\frac{k_1}{k_2}C(\boldsymbol{\theta},\dot{\boldsymbol{\theta}})\boldsymbol{e}(t)-\frac{E(t)}{k_2}\\&-\frac{k_3E(t)}{\|E(t)\|}-\hat{W}^TH(\boldsymbol{x})-\hat{F}(t).\end{aligned}\tag{16}$$

where k_1,k_2 are from (12), $k_3>\varepsilon_N$ is a robust gain parameter that confines the effect of the sign of $E(t)$, and $\boldsymbol{x}=[\boldsymbol{e}^T,\dot{\boldsymbol{e}}^T,\ddot{\boldsymbol{e}}^T]^T$. The network updating law is given by

$$\dot{\hat{W}}=\Psi H(\boldsymbol{x})E^T(t),\tag{17}$$

where Ψ is a prespecified positive-definite diagonal matrix. $\hat{W}^TH(\boldsymbol{x})$ is used to approximate

$$W^{*T}H(\boldsymbol{x})=F(t)+\Delta-\varepsilon(\boldsymbol{x}),\tag{18}$$

where W^{*T} is the ideal NN weights, and $\varepsilon(\boldsymbol{x})$ is the approximation error of the NN. The learning law for $\hat{F}(t)$ is

$$\begin{cases}\hat{F}(t)&=&\hat{F}(t-T)+k_4E(t),\ t>0,\\\hat{F}(t)&=&\mathbf{0},\ \forall t\in[-T,0],\end{cases}\tag{19}$$

where $k_4>0$ is the repetitive learning gain. The main result is summarized in the following theorem.

Theorem 1. For the exoskeleton dynamics (1) under *Properties* 1-3 and *Assumption* 1, when the control law (13), (16), (17), and the RLC law (19) are applied, the tracking error $\boldsymbol{e}(t)$ will converge to zero asymptotically, and all the signals of the closed-loop system are bounded.

Proof. Let

$$\widetilde{F}(t)=F(t)-\hat{F}(t).\tag{20}$$

Consider the Lyapunov function candidate

$$V(t)=V_1(t)+V_2(t)+V_3(t),\tag{21}$$

$$V_1(t)=E^T(t)M(\boldsymbol{\theta})E(t),\tag{22}$$

$$V_2(t)=k_2tr[\widetilde{W}^T(t)\Psi^{-1}\widetilde{W}(t)],\tag{23}$$

$$V_3(t)=\frac{k_2}{k_4}\int_{t-T}^{t}\widetilde{F}^T(\mu)\widetilde{F}(\mu)d\mu\tag{24}$$

where $\widetilde{W}=W^*-\hat{W}$. Then, the time derivative of $V(t)$ is

$$\dot{V}(t)=\dot{V}_1(t)+\dot{V}_2(t)+\dot{V}_3(t),\tag{25}$$

$$\dot{V}_1(t)=2E^T(t)M(\boldsymbol{\theta})\dot{E}(t)+E^T(t)\dot{M}(\boldsymbol{\theta})E(t),\tag{26}$$

$$\dot{V}_2(t)=2k_2tr[\widetilde{W}^T\Psi^{-1}\dot{\widetilde{W}}],\tag{27}$$

$$\dot{V}_3(t)=\frac{k_2}{k_4}[\widetilde{F}^T(t)\widetilde{F}(t)-\widetilde{F}^T(t-T)\widetilde{F}(t-T)].\tag{28}$$

First address $\dot{V}_1(t)$. Note that

$$\begin{aligned}&M(\boldsymbol{\theta})\dot{E}(t)=M(\boldsymbol{\theta})[k_1\dot{\boldsymbol{e}}(t)+k_2\ddot{\boldsymbol{e}}(t)]\\=&k_1M(\boldsymbol{\theta})\dot{\boldsymbol{e}}(t)+k_2M(\boldsymbol{\theta})\ddot{\boldsymbol{e}}(t)\\=&k_1M(\boldsymbol{\theta})\dot{\boldsymbol{e}}(t)+k_2[\boldsymbol{u}+F(t)+\Delta-C(\boldsymbol{\theta},\dot{\boldsymbol{\theta}})\dot{\boldsymbol{e}}(t)]\\=&k_1M(\boldsymbol{\theta})\dot{\boldsymbol{e}}(t)+k_2\left[\boldsymbol{u}+F(t)+\Delta\right.\\&\left.-C(\boldsymbol{\theta},\dot{\boldsymbol{\theta}})\frac{E(t)-k_1\boldsymbol{e}(t)}{k_2}\right]\\=&k_1M(\boldsymbol{\theta})\dot{\boldsymbol{e}}(t)+k_2[\boldsymbol{u}+F(t)+\Delta]\\&+k_1C(\boldsymbol{\theta},\dot{\boldsymbol{\theta}})\boldsymbol{e}(t)-C(\boldsymbol{\theta},\dot{\boldsymbol{\theta}})E(t).\end{aligned}\tag{29}$$

Substituting (29) into (26) renders to

$$\begin{aligned}\dot{V}_1(t)=&2E^T(t)\{k_1M(\boldsymbol{\theta})\dot{\boldsymbol{e}}(t)+k_2[\boldsymbol{u}+F(t)+\Delta]\\&+k_1C(\boldsymbol{\theta},\dot{\boldsymbol{\theta}})\boldsymbol{e}(t)-C(\boldsymbol{\theta},\dot{\boldsymbol{\theta}})E(t)\}+E^T(t)\dot{M}(\boldsymbol{\theta})E(t)\\=&2E^T(t)\{k_1M(\boldsymbol{\theta})\dot{\boldsymbol{e}}(t)+k_2[\boldsymbol{u}+F(t)+\Delta]\\&+k_1C(\boldsymbol{\theta},\dot{\boldsymbol{\theta}})\boldsymbol{e}(t)\}-2E^T(t)C(\boldsymbol{\theta},\dot{\boldsymbol{\theta}})E(t)\\&+E^T(t)\dot{M}(\boldsymbol{\theta})E(t)\\=&2E^T(t)\{k_1M(\boldsymbol{\theta})\dot{\boldsymbol{e}}(t)+k_2[\boldsymbol{u}+F(t)+\Delta]\\&+k_1C(\boldsymbol{\theta},\dot{\boldsymbol{\theta}})\boldsymbol{e}(t)\}+E^T(t)[\dot{M}(\boldsymbol{\theta})-2C(\boldsymbol{\theta},\dot{\boldsymbol{\theta}})]E(t).\end{aligned}\tag{30}$$

According to *Property* 2, (30) can be further simplified.

$$\begin{aligned}\dot{V}_1(t)=&2E^T(t)\{k_1M(\boldsymbol{\theta})\dot{\boldsymbol{e}}(t)+k_2[\boldsymbol{u}+F(t)+\Delta]\\&+k_1C(\boldsymbol{\theta},\dot{\boldsymbol{\theta}})\boldsymbol{e}(t)\}\\=&2k_1E^T(t)M(\boldsymbol{\theta})\dot{\boldsymbol{e}}(t)+2k_1E^T(t)C(\boldsymbol{\theta},\dot{\boldsymbol{\theta}})\boldsymbol{e}(t)\\&+2k_2E^T(t)[\boldsymbol{u}+F(t)+\Delta].\end{aligned}\tag{31}$$

Second, $\dot{V}_2(t)$ is addressed. By considering the NN updating law (17),

$$\dot{\widetilde{W}}=\dot{W}^*-\dot{\hat{W}}=-\dot{\hat{W}}=-\Psi H(\boldsymbol{x})E^T(t).\tag{32}$$

Combining (27) and (38), one gets

$$\begin{aligned}\dot{V}_2(t)=&2k_2tr[\widetilde{W}^T\Psi^{-1}(-\Psi H(\boldsymbol{x})E^T(t))]\\=&-2k_2tr[\widetilde{W}^TH(\boldsymbol{x})E^T(t)].\end{aligned}\tag{33}$$

Since [35]

$$tr[\widetilde{W}^TH(x)E^T(t)]=E^T(t)\widetilde{W}^TH(x),\tag{34}$$

it follows that

$$\dot{V}_2(t)=-2k_2E^T(t)\widetilde{W}^TH(x).\tag{35}$$

Third, $\dot{V}_3(t)$ is addressed. By virtue of *Lemma* 1 and (19), we can obtain

$$\begin{aligned}\dot{V}_3(t)=&\frac{k_2}{k_4}[2k_4\widetilde{F}^T(t)E(t)-k_4^2E^T(t)E(t)]\\=&-2k_2\widetilde{F}^T(t)E(t)-k_2k_4E^T(t)E(t).\end{aligned}\tag{36}$$

Subsequently, combination of (25), (31), (35), and (36) leads to

$$\begin{aligned}\dot{V}(t)=&\dot{V}_1(t)+\dot{V}_2(t)+\dot{V}_3(t),\\=&2k_1E^T(t)M(\boldsymbol{\theta})\dot{\boldsymbol{e}}(t)+2k_1E^T(t)C(\boldsymbol{\theta},\dot{\boldsymbol{\theta}})\boldsymbol{e}(t)\\&+2k_2E^T(t)[\boldsymbol{u}+F(t)+\Delta]-2k_2E^T(t)\widetilde{W}^TH(x)\\&-2k_2\widetilde{F}^T(t)E(t)-k_2k_4E^T(t)E(t).\end{aligned}\tag{37}$$

It is worthy of noticing from (18) that

$$F(t)+\Delta=W^{*T}H(\boldsymbol{x})+\varepsilon(\boldsymbol{x}).\tag{38}$$

Substituting the virtual control law (16) into (37) yields

$$
\begin{aligned}
&\dot{V}(t)\\
=&-2E^T(t)E(t)-2k_2k_3\|E(t)\|\\
&+2k_2E^T(t)[W^{*T}H(\boldsymbol{x})+\varepsilon(\boldsymbol{x})-\hat{W}^TH(\boldsymbol{x})+F(t)-\hat{F}(t)]\\
&-2k_2E^T(t)\widetilde{W}^TH(\boldsymbol{x})-2k_2\widetilde{F}^T(t)E(t)-k_2k_4E^T(t)E(t)\\
=&-2E^T(t)E(t)-2k_2k_3\|E(t)\|\\
&+2k_2E^T(t)[\widetilde{W}^TH(\boldsymbol{x})+\varepsilon(\boldsymbol{x})+\widetilde{F}(t)]\\
&-2k_2E^T(t)\widetilde{W}^TH(\boldsymbol{x})-2k_2\widetilde{F}^T(t)E(t)-k_2k_4E^T(t)E(t)\\
=&-2E^T(t)E(t)-2k_2k_3\|E(t)\|+2k_2E^T(t)\varepsilon(\boldsymbol{x})\\
&+2k_2E^T(t)\widetilde{F}(t)-2k_2\widetilde{F}^T(t)E(t)-k_2k_4E^T(t)E(t)\\
=&-2E^T(t)E(t)-2k_2k_3\|E(t)\|+2k_2E^T(t)\varepsilon(\boldsymbol{x})\\
&-k_2k_4E^T(t)E(t).
\end{aligned}
\tag{39}
$$

Further, using the Schwarz inequality

$$E^T(t)\varepsilon(\boldsymbol{x})\leq\|E(t)\|\cdot\|\varepsilon(\boldsymbol{x})\|, \tag{40}$$

we have

$$
\begin{aligned}
\dot{V}(t)\leq&-2E^T(t)E(t)-2k_2k_3\|E(t)\|-k_2k_4E^T(t)E(t)\\
&+2k_2\|E(t)\|\|\varepsilon(\boldsymbol{x})\|\\
<&-2E^T(t)E(t)-k_2k_4E^T(t)E(t)\\
&-2k_2\|E(t)\|(k_3-\varepsilon_N)
\end{aligned}
\tag{41}
$$

where the condition (10) is applied. By selecting k_3 such that $k_3-\varepsilon_N>0$,

$$\dot{V}(t)<-(2+k_2k_4)E^T(t)E(t)\leq 0, \tag{42}$$

implying that the CEF $E(t)$ will converge to zero asymptotically. The remaining work is to check the boundedness of all the signals involved in the closed-loop system. Integrating both sides of (41) yields

$$
\begin{aligned}
V(t)-V(0)<&-\int_0^t[2E^T(t)E(t)]du-\int_0^t[k_2k_4E^T(T)E(t)]du\\
&-\int_0^t[2k_2\|E(t)\|(k_3-\|\varepsilon_N\|)]du\\
=&-2\int_0^t[E^T(t)E(t)]du-k_2k_4\int_0^t[E^T(T)E(t)]du\\
&-2k_2\int_0^t[\|E(t)\|(k_3-\|\varepsilon_N\|)]du\\
<&\,\infty
\end{aligned}
\tag{43}
$$

Thus, $V(t)$ is bounded, which means that $E(t)\in L_\infty$, as θ_d is bounded in a practical dynamic system. $\hat{W}$ is bounded as W^* is a constant. $\hat{F}(t)$ is bounded with $\widetilde{F}(t)$ converging to zero. Hence, all signals are bounded. $\boldsymbol{e}(t)$ $\dot{\boldsymbol{e}}(t)$ converge to zero as the fact that $k_1>0$, $k_2>0$ and $k_4>0$. The proof of *Theorem* 1 is complete. ■

4 Simulation Results

An exoskeleton with two links is considered for simulation. Let m_i and l_i be the mass and length of joint i, d_i be the distance from joint $i-1$ to the center of mass of link i, I_i be the moment of inertia of link i about an axis coming out of the page passing through the center of mass of link i. The inertia nominal matrix, $M(\boldsymbol{\theta})$, the centrifugal and Coriolis nominal terms, $C(\boldsymbol{\theta},\dot{\boldsymbol{\theta}})$, and the gravity nominal vector, $G(\boldsymbol{\theta})$, are expressed as [41]

$$M(\boldsymbol{\theta})=\begin{bmatrix}M_{11}&M_{12}\\M_{21}&M_{22}\end{bmatrix}$$

$$C(\boldsymbol{\theta},\dot{\boldsymbol{\theta}})=\begin{bmatrix}C_{11}&C_{12}\\C_{21}&C_{22}\end{bmatrix}$$

$$G(\boldsymbol{\theta})=\begin{bmatrix}G_{11}\\G_{21}\end{bmatrix}$$

where

$$
\begin{aligned}
M_{11}=&m_1d_1^2+m_2(l_1^2+d_2^2+2l_1d_2\cos\theta_2)+I_1+I_2,\\
M_{12}=&m_2(d_2^2+l_1d_2\cos\theta_2)+I_2,\\
M_{21}=&M_{12},\\
M_{22}=&m_2d_2^2+I_2,\\
C_{11}=&-m_2l_1d_2\dot{\theta}_2\sin\theta_2,\\
C_{12}=&-m_2l_1d_2(\dot{\theta}_1+\dot{\theta}_2)\sin\theta_2,\\
C_{21}=&m_2l_1d_2\dot{\theta}_1\sin\theta_2,\\
C_{22}=&0,\\
G_{11}=&(m_1d_2+m_2l_1)g\cos\theta_1+m_2d_2g\cos(\theta_1+\theta_2),\\
G_{21}=&m_2d_2g\cos(\theta_1+\theta_2).
\end{aligned}
\tag{44}
$$

The parameters of the system dynamic are shown in Tab. 1. The moment of inertia $I_1=\frac{1}{3}m_1l_1^2$, $I_2=\frac{1}{12}m_2l_2^2$. The external disturbance and frictional forces $\Delta(t)=1+2||\boldsymbol{e}(t)||+3||\dot{\boldsymbol{e}}(t)||$, and the interactions between the wearer and exoskeleton are $F_1(t)=2\cos(2\pi t)$, $F_2(t)=2\sin(2\pi t)$. The desired training trajectories are given as

Table 1: Parameters of the system dynamic

m_1	2.6 kg
m_2	3.2 kg
1_1	25 cm
1_2	30 cm
d_1	12 cm
d_2	15 cm

$$
\begin{cases}
\theta_{d,1} &= \; 0.8+0.2\sin(2\pi t)\ rad,\\
\theta_{d,2} &= \; 1.2-0.2\cos(2\pi t)\ rad.
\end{cases}
\tag{45}
$$

The initial tracking error is chosen to be $e_1(0)=0.1$ rad, $e_2(0)=0.15$ rad. In addition, the centres of the RBF NN are chosen as $c_j=0.1\times j$, $j=0,\pm1,\pm2$ for link 1 and $c_j=0.2\times j$, $j=0,\pm1,\pm2$ for link 2. The width of the NN is chosen as $\sigma=1$ for both of the links. The initial weight values are all set to be zero. The parameters of the controller is shwon in Tab. 2

The tracking performance of the proposed controller is shown in Fig. 1 to Fig. 4. The convergence of the proposed controller scheme is clear.

Table 2: Parameters of the controller

k_1	10
k_2	1
k_3	10
k_4	5

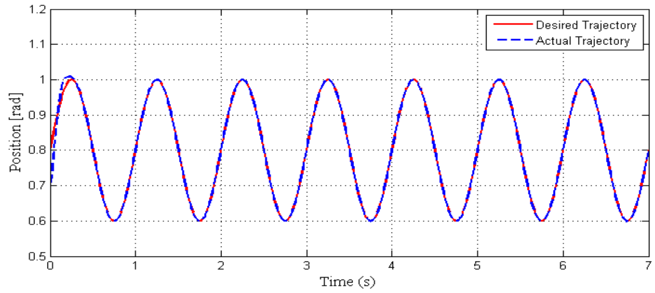

Fig. 1: Tracking performance of joint 1

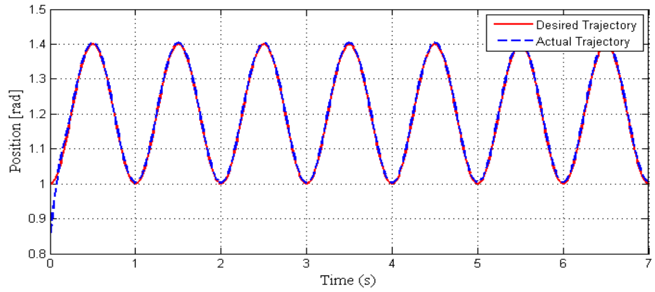

Fig. 2: Tracking performance of joint 2

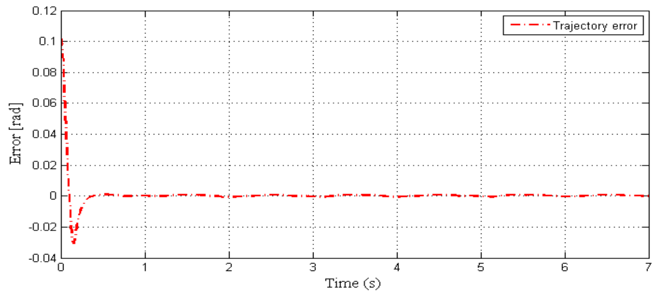

Fig. 3: Tracking error of joint 1

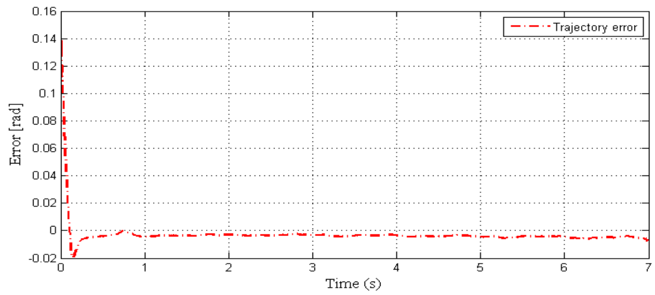

Fig. 4: Tracking error of joint 2

5 Conclusion

The neural networks control of lower limb exoskeleton for rehabilitation is studied. The convergence of the system tracking errors are investigated in a Lyapunov way. By making full use of the repetitiveness of the motion during rehabilitation therapy, an neural network controller with repetitive learning is proposed, where the repetitive learning part is to learn the periodic uncertainties, and the NN part is to learn the non-periodic uncertainties. Simulations reveal that the tracking performance can be efficient by learning the involved periodic uncertainties in a repetitive way. Our next research phase is to test the proposed control scheme experimentally.

References

[1] Z. Zhang, Q. Fang, and X. Gu, "Objective assessment of upper-limb mobility for poststroke rehabilitation," *IEEE Trans. Biomed. Eng.*, vol. 63, no. 4, pp. 859-868, Apr. 2016.

[2] G. B. Prange, M. J. A. Jannink, C. G. M. Groothuis-Oudshoorn, H. J. Hermens, and M. J. IJzerman, "Systematic review of the effect of robot-aided therapy on recovery of the hemiparetic arm after stroke," *J. Rehabil. Res. Devel.*,vol. 43, no. 2, pp. 171-184, Mar. 2006.

[3] S. Jezernik, G. Colombo, and M. Morari, "Automatic gait-pattern adaptation algorithms for rehabilitation with a 4-DOF robotic orthosis," *IEEE Trans. Robot. Autom.*, vol. 20, no. 3, pp. 574-582, June 2004.

[4] R. Riener, L. Lünenburger, S. Jezernik, M. Anderschitz, G. Colombo, and V. Dietz, "Patient-cooperative strategies for robot-aided treadmill training: first experimental results," *IEEE Trans. Neural Syst. Rehabil. Eng.*, vol. 13, no. 3, pp. 380-394, Sept. 2005.

[5] Y. Yang, M. Lei, and D. Huang, "Development and repetitive learning control of lower limb exoskeleton driven by electro-hydraulic actuators," *IEEE Trans. Ind. Electron.*, in press, 2016. DOI:10.1109/TIE.2016.2622665.

[6] M. Khezri and M. Jahed, "A neuro-fuzzy inference system for sEMG-based identification of hand motion commands," *IEEE Trans. Ind. Electron.*,vol. 58, no. 5, pp. 1952-1960, May 2011.

[7] L. Lünenburger, G. Colombo, and R. Riener, "Biofeedback for robotic gait rehabilitation," *J. NeuroEng. Rehabil.*, vol. 4, no. 1, pp. 1-11, Jan. 2007.

[8] Z. Ma, P. Ben-Tzvi, and J. Danoff, "Hand rehabilitation learning system with an exoskeleton robotic glove," *IEEE Trans. Neural Syst. Rehabil. Eng.*, vol. 24, no. 12, pp. 1323-1332, Dec. 2016.

[9] A. Frisoli, C. Loconsole, D. Leonardis, F. Banno, M. Barsotti, C. Chisari, and M. Bergamasco, "A new gaze-BCI-driven control of an upper limb exoskeleton for rehabilitation in real-world tasks," *IEEE Trans. Syst. Man Cybern. Part C-Appl. Rev.*, vol. 42, no. 6, pp. 1169-1179, Nov. 2012.

[10] Y. Mao and S. K. Agrawal, "Design of a cable-driven arm exoskeleton (CAREX) for neural rehabilitation," *IEEE Trans. Robot.*, vol 28, no. 4, pp. 922-931, Aug. 2012.

[11] A. M. Dollar and H. Herr, "Lower extremity exoskeletons and active orthoses: Challenges and state-of-the-art," *IEEE Trans. Robotics*, vol. 24, no. 1, pp. 144-158, Feb. 2008.

[12] B. Ugurlu, M. Nishimura, K. Hyodo, M. Kawanishi, and T. Narikiyo, "Proof of concept for robot-aided upper limb rehabilitation using disturbance observers," *IEEE T. Hum.-Mach. Syst.*, vol. 45, no. 1, pp. 110-118, Feb. 2015.

[13] U. Keller, H. J. A. Hedel, V. K. Marganska, and R. Riener, "ChARMin: the first actuated exoskeleton robot for pediatric arm rehabilitation," *IEEE-ASME Trans. Mechatron.*, vol. 21, no. 5, pp. 2201-2213, Oct. 2016.

[14] K. Kiguchi and Y. Hayashi, "An EMG-based control for an upper-limb power-assist exoskeleton robot," *IEEE Trans. Syst. Man Cybern. Part B-Cybern.*, vol. 42, no. 4, pp. 1064-1071, Aug. 2012.

[15] G. A. Ollinger, J. E. Colgate, M. A. Peshkin, and A. Goswami, "Inertia compensation control of a one-degree-of-freedom ex-

oskeleton for lower-limb assistance: Initial experiments," *IEEE Trans. Neural Syst. Rehabil. Eng.*, vol. 20, no. 1, pp. 68-77, 2012.

[16] W. He, Y. Dong, and C. Sun, "Adaptive neural impedance control of a robotic manipulator with input saturation," *IEEE Trans. Syst., Man, Cybern., Syst.*, vol. 46, no. 3, pp. 334-344, Mar. 2016.

[17] L. Wang et al., "Energy-efficient SVM learning control system for biped walking robots," *IEEE Trans. Neural Netw. Learn. Syst.*, vol. 24, no. 5, pp. 831-837, May 2013.

[18] K. Tanghe, A. Harutyunyan, E. Aertbeliën, F. D. Grooté, J. D. Schutter, P. Vrancx, and A. Nowé, "Predicting seat-Off and detecting start-of-assistance events for assisting sit-to-stand with an exoskeleton," *IEEE Robot. Autom. Mag.*, vol. 1, no. 2, pp. 792-799, July 2016.

[19] X. Chen, Y. Zeng, and Y. Yin, "Improving the transparency of an exoskeleton knee joint based on the understanding of motor intent using energy kernel method of EMG," *IEEE Trans. Neural Syst. Rehabil. Eng.*, in press, DOI:10.1109/TNSRE.2016.2582321.

[20] Z. Li, Z. Huang, W. He, and C. Su, "Adaptive impedance control for an upper limb robotic exoskeleton using biological signals," *IEEE Trans. Ind. Electron.*, vol. 64, no. 2, pp. 1664-1674, Feb. 2017.

[21] Z. Liu, C. Chen, Y. Zhang, and C. L. P. Chen, "Adaptive neural control for dual-arm coordination of humanoid robot with unknown nonlinearities in output mechanism," *IEEE Trans. Cybern.*, vol. 45, no. 3, pp. 521-532, Mar. 2015.

[22] W. He, S. S. Ge, Y. Li, E. Chew, and Y. S. Ng, "Neural network control of a rehabilitation robot by state and output feedback," *J. Intell. Robot. Syst.*, vol. 80, no. 1, pp 15-31, Oct. 2015.

[23] F. Rossomando, C. Soria, and R. Carelli, "Neural network-based compensation control of mobile robots with partially known structure," *IET Control Theory Appl.*, vol. 6, no. 12, pp. 1851-1860, Aug. 2012.

[24] Y. Kim and F. Lewis, "Optimal design of CMAC neural-network controller for robot manipulators," *IEEE Trans. Syst., Man, Cybern. C, Appl. Rev.*, vol. 30, no. 1, pp. 22-31, Feb. 2000.

[25] J. Xu, and R. Yan, "On repetitive learning control for periodic tracking tasks," *IEEE Trans. Autom. Control*, vol. 51, no. 11, pp. 1842-1848, Nov. 2006.

[26] D. Huang, J. Xu, S. Yang, and X. Jin, "Observer based repetitive learning control for a class of nonlinear systems with non-parametric uncertainties," *Int. J. Robust Nonlinear Control*, vol. 25, pp. 1214-1229, 2015.

[27] M. Sun and S. S. Ge, "Adaptive repetitive control for a class of nonlinearly parametrized systems," *IEEE Trans. Autom. Control*, vol. 51, no. 10, pp. 1684-1688, Oct. 2006.

[28] W. E. Dixon, E. Zergeroglu, D. M. Dawson, and B. T. Costic "Repetitive learning control: a lyapunov-based approach," *IEEE Trans. Syst. Man Cybern. Part B-Cybern.*, vol. 32, no. 4, pp. 538-545, Aug. 2002.

[29] X. Li, T. W. S. Chow, J. K. L. Ho, and H. Tan, "Repetitive learning control of nonlinear continuous-time systems using quasi-sliding mode," *IEEE Trans. Control Syst. Technol.*, vol. 15, no. 2, pp. 369-374, Mar. 2007.

[30] M. Sun, S. S. Ge, and I. M. Y. Mareels, "Adaptive repetitive learning control of robotic manipulators without the requirement for initial repositioning," *IEEE Trans. Robot.*, vol. 22, no. 3, pp. 563-568, June 2006.

[31] Y. Hamada and H. Otsulu, "Repetitive learning control system using disturbance observer for head positioning control system of magnetic disk drives," *IEEE Trans. Magn.*, vol. 32, no. 5, pp. 5019-5021, Sep. 1996.

[32] T. J. Manayathara, T. C. Tsao, J. Bentsman, and D. Ross, "Rejection of unknown periodic load disturbances in continuous steel casting process using learning repetitive control approach," *IEEE Trans. Control Syst. Technol.*, vol. 4, no. 3, pp. 259-265, May 1996.

[33] S. Scalzi, S. Bifaretti, and C. M. Verrelli, "Repetitive learning control design for LED light tracking," *IEEE Trans. Control Syst. Technol.*, vol. 23, no. 3, pp. 1139-1146, May 2015.

[34] K. Zhou and D. Wang, "Digital repetitive learning controller for three-phase CVCF PWM inverter," *IEEE Trans. Ind. Electron.*, vol. 48, no. 4, pp. 820-830, Aug. 2001.

[35] G. Feng, "A compensating scheme for robot tracking based on neural networks," *Robot. Auton. Syst.*, vol. 15, pp. 199-206, 1995.

[36] R. Selmic and F. Lewis, "Deadzone compensation in motion control systems using neural networks," *IEEE Trans. Autom. Control*, vol. 45, no. 4, pp. 602-613, Apr. 2000.

[37] S. Seshagiri and H. K. Khalil, "Output feedback control of nonlinear systems using RBF neural networks," *IEEE Trans. Neural Netw.*, vol. 11, no. 1, pp. 69-79, Jan. 2000.

[38] Y. Zuo, Y. Wang, X. Liu, S. X. Yang, L. Huang, X. Wu, and Z. Wang, "Neural network robust H_∞ tracking control strategy for robot manipulators,," *Appl. Math. Model.*, vol. 34, no. 7, pp. 1823-2838, 2010.

[39] J. X. Xu and R. Yan, "Synchronization of chaotic systems via learning control," *Int. J. Bifurcation Chaos*, vol. 15, no. 12, pp. 4035-4041, 2005.

[40] N. E. Cotter, "The Stone-Weierstrass Theorem and Its Application to Neural Networks," *IEEE Trans. Neural Networks*, vol. 1, no. 4, pp. 290-295, 1990.

[41] W. He, Y. Chen, and Z. Yin, "Adaptive neural network control of an uncertain robot with full-state constraints," *IEEE Trans. Cybern.*, vol. 46, no. 3, pp. 620-629, Mar. 2016.